Geopersia 2021, 11(1): 153-168
DOI: 10.22059/GEOPE.2020.301568.648549

RESEARCH PAPER

Reservoir lithofacies modeling using well logs and seismic data based on Sequential Indicator Simulations and Probability Perturbation Method in a Bayesian framework

Mohamadreza Shad salanghouch, Mohammad Emami Niri**

Institute of Petroleum Engineering, College of Engineering, University of Tehran, Tehran, Iran

Received: 25 April 2020, Revised: 01 September 2020, Accepted: 14 September 2020

Abstract
In this paper, an inverse framework based on Bayes' theorem is suggested for integrating well logs and seismic data into the reservoir lithofacies modeling process. The proposed method is based on the combination of the Sequential Indicator Simulation (SIS), and a stochastic optimization method (i.e. the Probability Perturbation Method (PPM)). SIS is used to calculate the conditional probability of presence or absence of lithofacies indicators in each grid-block, and PPM is applied to update (perturb) the conditional probability used in SIS. A notable innovation presented in this study is using the Genetic algorithm' crossover operator to increase the PPM exploitation capability. To demonstrate the efficiency of our proposed approach, the results of its application on a 3D test model is compared with outcomes of two commonly-used constraining approaches on SIS technique. Qualitative and quantitative analysis of the obtained results on 3D test model reveals a (23.8)% and (16.98)% (on average) improvement in consistency of the lithofacies models generated using the proposed approach with the reference lithofacies model over the employed Vertical Probability Trend and the Seismic Probability Trend constraining approaches on SIS, respectively. Besides, the obtained results show that implementing the crossover operator leads to a 4.56% improvement in matching of the constructed lithofacies models with the reference model.

Keywords: Lithofacies modeling, Seismic data, Probability Perturbation Method, Sequential Indicator Simulation, Bayes' theorem

Introduction

Understanding reservoir behavior in the past and present, and forecast its future performance is an essential part of hydrocarbon reservoir management. This can be achieved through static modeling and dynamic simulation of the reservoir (Koneshloo et al., 2017). 3D static modeling of hydrocarbon reservoirs includes a description of the spatial distribution of its geological and petrophysical properties, such as geological lithofacies, porosity, permeability, and fluids saturation (Grana et al., 2012; Zhang & Zhang, 2017; Tewari & Dwivedi, 2019). The simultaneous integration of available datasets (geological, seismic, and engineering data) for the estimation of reservoir properties often requires solving an inverse problem. This requires the unknown parameters (spatial distribution of reservoir properties) to be considered as random variables (Caers & Hoffman, 2006; Adelu et al., 2019). Considering the limitations of different datasets, it is difficult to determine the unknown parameters uniquely (Abdelmaksoud et al., 2019). Consequently, the uncertainty in the process of reservoir modeling is inevitable

* Corresponding author e-mail: emami.m@ut.ac.ir

(Hoffman, 2005; El khadragy et al., 2017; Tang et al., 2019). One of the conventional methods for handling this uncertainty is to build several equiprobable realizations using geostatistical simulation approaches (Strebelle, 2002; Doyen, 2007; Kim et al., 2018). Although these methods are often fast for generating several models, the results are only compatible with the pre-existing measured points. Also, these data points are often insufficient for generating realistic reservoir models (Emami Niri, Lumley, 2017; Elzain et al., 2020). For building close-to-real reservoir models, different datasets must be combined optimally and logically in the modeling process (Ravalec-Dupin et al., 2011; Emami Niri, Lumley, 2015). Seismic data due to its extensive areal coverage can be useful not only in identifying the geometry and framework of geological structures but also in estimating reservoir properties at unsampled locations (Doyen, 2007; Mondol, 2010; Emami Niri, 2018). Many probabilistic and deterministic approaches have been employed to integrate seismic data in the process of estimating the reservoir lithofacies and petrophysical properties (Bosch et al., 2010; Emami Niri, Lumley, 2016; Abdel-Fattah et al., 2020). These approaches can be divided into three major categories: i) establishing deterministic relationships between seismic attributes (e.g. P-wave velocity and acoustic impedance) and the reservoir properties (lithofacies or porosity) at well locations and employing these relationships in estimating reservoir properties at unsampled locations (Angeleri & Carpi, 2006); ii) using seismic data as a secondary or guiding data in a geostatistical estimation/simulation technique (Emami Niri & Lumley, 2013), and iii) the seismic matching loop approach which was initially introduced by Bornard et al. (2005).

To date, several researches have been performed on integrating well and seismic data in the reservoir geological and petrophysical properties modeling process. For example, Grana et al. (2010) proposed an approach aimed at integrating seismic amplitude data in modeling lithofacies and petrophysical properties (e.g., porosity and net-to-grass). They used Probability Perturbation Method (PPM) as a stochastic optimization algorithm to perturb lithofacies models to reach a better consistency with available seismic data. Ravalec-Dupin et al. (2011) used the Gradual Deformation Method (GDM) to update a set of reservoir lithofacies models to achieve a better match with P-wave acoustic impedance data. They implemented Particle Swarm Optimization (PSO) to find the optimal value of the GDM deformation parameter. Emami Niri and Lumley (2015) used an approach which can be classified as a seismic matching loop approach. They first generated a set of geomodels coherent with litho-log and P-wave impedance data. Then, they updated these geomodels to reach a better consistency with both P- and S-wave impedance data simultaneously. The optimization algorithm used to minimize the defined objective function was a multi-objective optimization algorithm (i.e. NSGA2).

In this research, an approach is proposed to integrate well-logs and seismic data into reservoir lithofacies modeling process. This approach is a combination of the Sequential Indicator Simulation (SIS) (Journel & Gomez-Hernandez, 1993) and PPM (Caers & Hoffman, 2006) within the Bayes' Theorem framework (Besag & Green, 1993). SIS determines a discrete probability distribution function by calculating the conditional probabilities of the lithofacies indicators' presence. By sampling this distribution function, a lithofacies indicator is assigned to each grid block (Hoffman & Caers, 2003). The conditional probabilities are calculated relative to all available datasets. The calculation of this conditional probability relative to well-log data depends on the distance between the unsampled locations and the well locations, the spatial correlation range (variogram range), and the prior distribution function (Grana et al., 2011). Updating these conditional probabilities of lithofacies indicators' presence in each grid block relative to seismic data is performed based on PPM. The combination of conditional probabilities relative to two datasets leads to the determination of a new probability distribution function. Sampling the new derived probability distribution function results in generating a reservoir lithofacies model consistent with well-logs and seismic data (Grana & Della Rosa, 2010; Grana et al., 2012). The number of unsampled points in a reservoir model framework can

be very high. As a result, it is very time-consuming to calculate the conditional probabilities of the lithofacies indicators occurrence relative to the seismic data for each grid block. PPM can solve this issue by perturbing the conditional probabilities, and changing only one parameter (Ravalec-Dupin et al., 2011). As a result, it is deemed as very efficient and practical approach. In fact, PPM by updating the presence probability of lithofacies indicator in every grid block modifies the reservoir model to be more consistent with seismic data while maintaining its consistency with well data (Caers & Hoffman, 2006). A general workflow of the proposed approach is shown in Figure 1.

The approach introduced in this research can be considered as an optimization algorithm that aims at finding the optimal reservoir lithofacies model consistent with well-logs and seismic data. A robust optimization algorithm must be able to explore the search space to find the global best solution. To achieve this goal, the algorithm must make good use of Exploration and Exploitation capabilities (Blum & Roli, 2003; Kar, 2016; Abdel-Basset et al., 2018). An algorithm's Exploration (diversification) capability is its ability to detect new areas in the search space to get out of local optima. This capability is created by inserting random operators in the algorithm (Binitha & Sathya, 2012). For example, in the genetic optimization algorithm, the mutation operator is responsible for the implementation of this feature (Agarwal & Srivastava, 2018). An algorithm's Exploitation (intensification) capability is its ability to use best found solutions to create better ones. The purpose of using this feature is to pay more attention to better solutions and hope to improve them to achieve the best global answer (Khajehzadeh et al., 2011; Abdel-Basset et al., 2018). The crossover operator combines best obtained solutions with current solutions to enhance genetic algorithm's Exploitation capability (Garg, 2016; Agarwal & Srivastava, 2018). One of the most important features of a robust optimization algorithm is to create the right balance between these two capabilities. Otherwise, the algorithm's ability to converge to the global best solution will be reduced (Crawford et al., 2017). If the Exploration capability overcomes the Exploitation, the searching methodology will be a random search, which results in divergence. On the other hand, if the Exploitation capability overcomes the Exploration, the algorithm will be trapped in a limited area of the search space and will find the local optimum of that specific area (Khormouji et al., 2014).

In this research, SIS technique is used to generate different lithofacies models by changing the random seed. Selection of random seeds is performed in an entirely random manner. As a result, SIS with generating various lithofacies models (solutions) aims at enhancing the proposed algorithm's exploration capability.

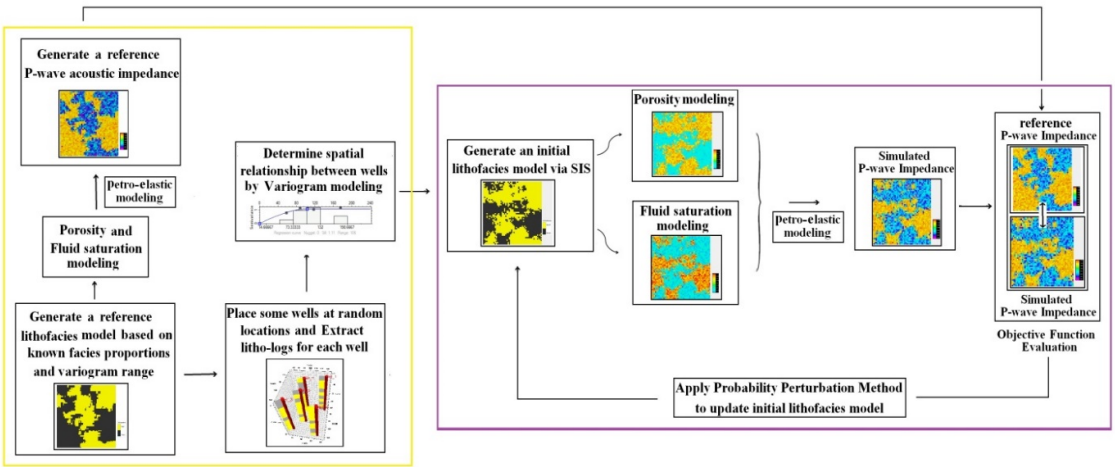

Figure 1. A schematic view for an application of the proposed approach on a synthetic case study. The yellow box illustrates the steps of generating a reference model and corresponding datasets, and the purple box shows the steps of a seismic matching loop based on PPM

Once a better lithofacies model is generated, it will be used as an initial starting model in the next iteration step. In other words, this substitution aims at intensifying the exploitation capability of the proposed algorithm. Investigations have shown that the exploitation ability of PPM in generating lithofacies models coherent with seismic data is not acceptable. One way to improve this ability is to use the crossover operator from the genetic algorithm. The key innovation of this research is to combine crossover operator with PPM to enhance the Exploitation capability of the algorithm.

Theory

Bayes' theorem

Integrating well and seismic data into the reservoir lithofacies modeling process could be addressed in a stochastic framework in which the desired properties are considered as random variables. The Bayes' theorem provides a suitable framework for solving such problems by sampling from a posterior distribution function. By considering two different datasets (d_1 and d_2), the posterior distribution ($f(m|d_1, d_2)$) can be achieved from equation (1) (Besag & Green, 1993):

$$f(m|d_1, d_2) = \frac{f(d_1, d_2|m)f(m)}{f(d_1, d_2)} \sim \frac{f(d_1|m)f(d_2|m)}{f(d_1, d_2)} f(m) \quad (1)$$

d_1 (well-based data) could only be measured at limited number of points. The relationship between d_1 and model parameter (m) is linear or pseudo-linear. d_2 (seismic data) has a nonlinear relationship with m. $f(m)$ (prior distribution) characterizes the dependency of parameters and hence constrains the obtained solutions. $f(d|m)$ (likelihood density function) considers the relationship between the observed data and each generated model. This term takes into account the generated model and measurement error. In the absence of any error, the relationship between m and d_2 can be expressed through the forward model (g):

$$d_2 = g(m) \quad (2)$$

Determination of $f(d_1, d_2)$ depends on the prior distribution and the forward model. The Bayesian inverse methods aim at sampling from the posterior distribution function. Traditional sampling methods like Markov Chain Monte Carlo (MCMC) method in sampling from the posterior distribution are applicable but very time-consuming. To overcome this problem, the practical PPM approach can be used. This method is based on two principles:

Using fast non-iterative sequential simulation for sampling from the posterior distribution function.

Using the pre-posterior terms instead of the likelihoods.

Sampling the prior

Regardless of the parameters' nature (continuous or discrete), the presence or absence of a specific event (a specific lithofacies indicator) in each grid block can be expressed through equation (3):

$$I(z) = \begin{cases} 1 & if\ the\ "event"\ occures\ at\ z \\ 0 & otherwise \end{cases} \quad (3)$$

The unknown model parameters are obtained by specifying the indicator (I) in each grid block. Fast and non-iterative sequential simulation can be used for sampling from the prior

distribution after visiting all unsampled locations in an entirely random path. Sequential simulation is defined based on the following prior distribution decomposition (Caers & Hoffman, 2006):

$$f(m) = prob\{I(z_1) = 1\} * prob\{I(z_2) = 1|i(z_1)\} * \dots * prob\{I(z_N) = 1|i(z_1), \dots, i(z_{N-1})\} \quad (4)$$

Several models can be generated by sampling from the prior distribution function by changing the random seed. The random seed produces a random path in which the grid blocks are visited. The prior distribution also can be expressed as statistical information (such as mean or covariance).

Sampling the posterior

As formulated in equation (1), conditioning the prior distribution to d_1 and d_2 determines the posterior distribution function. The posterior distribution function unlike the prior one matches with both datasets. The sequential simulation can sample from this posterior distribution function according to the following equations (Caers & Hoffman, 2006):

$$f(m|d_1, d_2) = prob\{I(z_1) = 1|\{i(z_\alpha), \alpha = 1, \dots, n\}, d_2\} * prob\{I(z_2) = 1|i(z_1), \{i(z_\alpha), \alpha = 1, \dots, n\}, d_2\} * \dots * prob\{I(z_\alpha) = 1|i(z_1), \dots, i(z_{N-1}), \{i(z_\alpha), \alpha = 1, \dots, n\}, d_2\} \quad (5)$$

$$d_1 = \{i(z_\alpha), \alpha = 1, \dots, n\} \quad (6)$$

$$d_2 = g(m) = g(I(z_1), I(z_2), \dots, I(z_N)) \quad (7)$$

Sampling from $f(m|d_1, d_2)$ is equivalent to the sampling from the following univariate conditional probability set (Hoffman & Caers, 2003):

$$prob\{I(z_i) = 1|i(z_1), \dots, i(z_{i-1}), \{i(z_\alpha), \alpha = 1, \dots, n\}, d_2\} = prob(A_j|B_j, C) \quad (8)$$

$$A_j = \{I(z_i) = 1\} \quad (9)$$

$$B_j = \{i(z_1), \dots, i(z_{i-1}), \{i(z_\alpha), \alpha = 1, \dots, n\}, d_2\} \quad (10)$$

$$C = d_2 \quad (11)$$

Since it is complicated process to determine $prob(A_j|B_j, C)$ explicitly, it is decomposed into two pre-posterior terms of $prob(A_j|B_j)$ and $prob(A_j|C)$, by using the "tau model" (Journel, 2002):

$$prob(A_j|B_j, C) = \frac{1}{1+x} \quad (12)$$

$$\frac{x}{a} = \left(\frac{b}{a}\right)^{\tau_1} * \left(\frac{c}{a}\right)^{\tau_2} \quad (13)$$

$$b = \frac{1 - prob(A_j|B_j)}{prob(A_j|B_j)} \quad (14)$$

$$c = \frac{1 - prob(A_j|C)}{prob(A_j|C)} \quad (15)$$

$$a = \frac{1 - prob(A_j)}{prob(A_j)} \quad (16)$$

τ_1 and τ_2 are datasets weights. With a known $prob(A_j)$, the problem of determining the

$prob(A_j|B_j, C)$ can be split into determining of $prob(A_j|B_j)$ and $prob(A_j|C)$.

Probability Perturbation Method

The pre-posterior distribution function $prob(A_j|B_j)$ expresses the conditional probability of the occurrence of A_j relative to previously simulated grid blocks and d_1. The conditional probability of occurrence A_j event in i'th grid block is calculated from equation (17) (Grana et al., 2012):

$$P(A_j|B_j) = P(A_j) + \sum_{i=1}^{N-1} \lambda_i \, (i(z_i, A_j) - P(A_j)) \quad (17)$$

Where the prior probability of occurrence A_j, the I-value (0 or 1) at the location z_i and the kriging weights are denoted by $P(A_j)$, $i(z_i, A_j)$ and λ_i, respectively. Given $prob(A_j|B_j)$ value in each grid block and considering a random seed (rs), it is possible to generate an initial starting realization $I_B^{(rs)} = \{i_B^{(rs)}(z_1), i_B^{(rs)}(z_2), \dots, i_B^{(rs)}(z_N)\}$ using the sequential simulation. The subscript B shows that this realization is only consistent with d_1 and has not yet been matched with d_2. To construct a model that is compatible with both data sources, each grid block needs to be sequentially sampled from the $prob(A_j|B_j, C)$. However, the $prob(A_j|B_j, C)$ is unknown, since $prob(A_j|C)$ is not calculated yet. To match the initial realization with d_2, the PPM performs a stochastic search to find $prob(A_j|C)$. It is very time-consuming to calculate $prob(A_j|C)$ for each grid block directly because the number of grid blocks can be too high. For tackling this issue, PPM can obtain $prob(A_j|C)$, only by modifying one parameter (r_c) (Hoffman & Caers, 2003):

$$prob(A_j|C) = prob(I(z_i) = 1|C) = (1 - r_c) * I_B^{(rs)}(z_i) + r_c * prob(A_j) \quad (18)$$

The r_c is the PPM deformation parameter varying in the range of [0,1]. $prob(A_j|C)$ can be determined for a specific value of r_c and a given initial model $I_B^{(rs)}$. Using equation (18) makes it possible to reduce an N-parameter problem into a problem with one parameter (r_c). r_c is not associated with the spatial location of grid blocks. Finding the optimal value of the deformation parameter r_c leads to the development of the optimal pre-posterior probability distribution $prob(A_j|C)$ and, consequently, the optimal $prob(A_j|B_j, C)$. Finally, a model with a proper consistency with both data sources can be obtained via sampling from $prob(A_j|B_j, C)$. For further information, refer to the Caers and Hoffman (2006).

Petro-elastic model

The petro-elastic model usually consists of a series of empirical or theoretical relations that links the geological and petrophysical parameters such as lithofacies, porosity, and fluid saturation to the seismic/elastic properties like P- and S-wave velocities and impedances (Churanova, 2018). For each grid block, the rock contains a solid matrix and pores filled by reservoir fluids. It is then replaced by a hypothetical continuous medium with average elastic properties (Mavko et al., 1998). The petro-elastic model applied in this research, estimates the dry rock bulk (K_{dry}) and shear (G_{dry}) moduli for each lithofacies indicator by the following equations introduced by Nur *et al.,* (1998):

$$K_{dry} = K_m\left(1 - \frac{\varphi}{\varphi_c}\right) \quad (19)$$

$$G_{dry} = G_m\left(1 - \frac{\varphi}{\varphi_c}\right) \quad (20)$$

Where the bulk and shear moduli of the rock minerals are denoted by K_m and G_m, respectively. φ_c is the critical porosity. Many factors such as mineral composition, diagenesis, pore shape, and burial history can affect the elastic properties of a dry rock (Ravalec-Dupin *et al.,* 2011). In this research, to calculate the saturated rock bulk (K_{sat}) and shear (G_{sat}) moduli, it is assumed that the Gassmann equations (Eq.21, 22) (Gassmann, 1951) is suitable for reservoir condition.

$$K_{sat} = K_{dry} + \frac{\left(1 - \frac{K_{dry}}{K_m}\right)^2}{\frac{\varphi}{K_f} + \frac{1-\varphi}{K_m} + \frac{K_{dry}}{K_m^2}} \quad (21)$$

$$G_{sat} = G_{dry} \quad (22)$$

The bulk modulus of fluid (K_f) can be estimated from wood's formula (wood, 1941):

$$\frac{1}{K_f} = \sum_{i=1}^{3}\frac{S_i}{K_i} = \frac{S_o}{K_o} + \frac{S_g}{K_g} + \frac{S_w}{K_w} \quad (23)$$

K_f depends on the pore pressure and fluid' saturations, so it needs to be defined at initial reservoir condition. Subscripts o, g, and w respectively represent oil, gas, and water. In the petro-elastic model designed in this research, it is assumed that a two-phase fluid (water and oil) fills the pore spaces. Gassmann's equations are reliable as long as the pore distribution is isotropic and the rock matrix is homogeneous (Ravalec-Dupin *et al.,* 2011). The density of the saturated rock is defined as a linear combination of matrix and fluid density as follows:

$$\rho = (1-\varphi)\rho_m + \varphi\left(s_o\rho_o + s_w\rho_w + s_g\rho_g\right) \quad (24)$$

Finally, the velocity and acoustic impedance of P- and S-waves propagating in the reservoir are obtained from the following well-known relationships:

$$V_p = \sqrt{\frac{k_{sat} + \frac{4}{3}G_{sat}}{\rho}} \quad (25)$$

$$V_s = \sqrt{\frac{G_{sat}}{\rho}} \quad (26)$$

$$I_p = \rho V_p \quad (27)$$

$$I_s = \rho V_s \quad (28)$$

It should be noted that the petro-elastic model used in this research is a deterministic model formulated in terms of equations. However, this model can also be generalized to a probabilistic model expressed in terms of probability density functions (e.g., Mavko & Mukerji, 1998).

Methodology

In this research, an approach based on geostatistical techniques within the Bayes' theorem framework is introduced. The prior distribution function is considered as lithofacies proportions reported at borehole locations. The conditional probability of the presence of j'th lithofacies indicator relative to well-log data (B) and P-wave acoustic impedance data (C) are denoted by

$prob(A_j|B_j)$ and $prob(A_j|C)$, respectively. The detailed description of the proposed approach is shown in Figure 2.

The crossover operator combines the current lithofacies model with the lowest objective function value hopefully to generate a lithofacies model with a lower objective function value. The lowest objective function value is associated with the lithofacies model which has the best match to both well logs and seismic data. The crossover operator used in this research is the uniform crossover.

The objective function is defined in a least-square form (Eq.29). This function measures the sum of the differences between observed and simulated P-wave acoustic impedances in each grid block.

$$J(x) = \sum_{i}^{N} \frac{\left(Ip_i^{sim}(x) - Ip_i^{obs}\right)^2}{\left(\sigma_{Ip}^{obs}\right)^2} \tag{29}$$

Where x is the unknown reservoir property (lithofacies indicator), N is the total number of grid blocks. Ip^{sim} and Ip^{obs} are simulated and observed P-wave acoustic impedances. The observed P-wave acoustic impedance variance is denoted by $\sigma_{\mathrm{Ip}}^{\mathrm{obs}}$.

Test model

In this section, an application of the proposed approach to generate optimum reservoir lithofacies model is presented on a 3D test model. The generated reference lithofacies model consists of 55% (clean) sand and 45% shaly sand (Figure 3). This 3D model contains 17*17*10 grid blocks (2890 total) with 15*15*6 m^3 dimensions. The distributions of sand and shaly sand are obtained based on SIS technique using spherical variogram parameters with the range of 130m horizontally and 6m vertically for both lithofacies types. The constructed reservoir lithofacies model (Figure 3) is considered as the true reservoir lithofacies model for this test example. Afterwards, five pseudo-wells are placed at random positions within the reservoir framework. Synthetic litho-logs are produced by extracting lithofacies types from grid blocks which are intersected by wells.

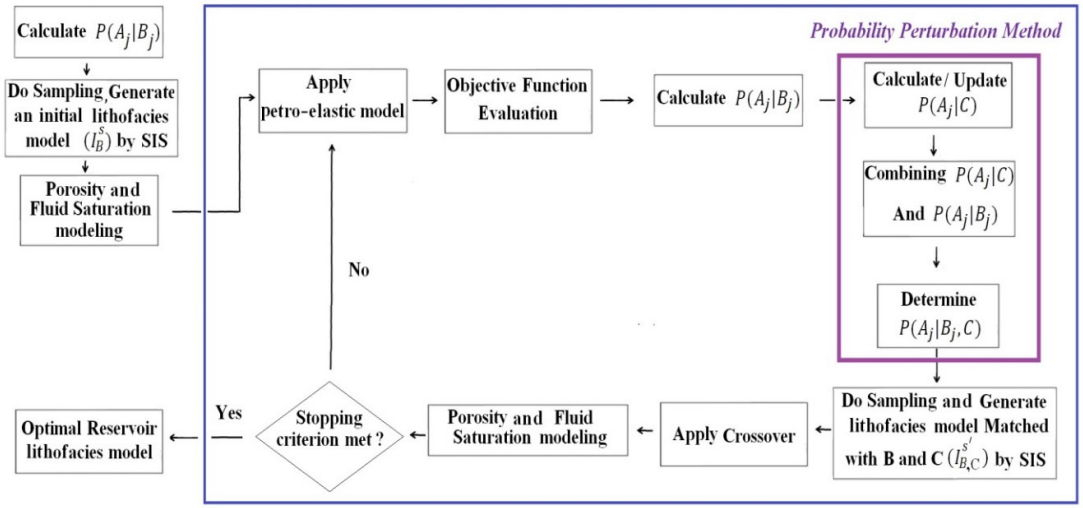

Figure 2. A Flow chart illustrating the steps of the proposed approach in generating/perturbing the reservoir lithofacies models consistent with B (litho-logs) and C (P-wave impedance) datasets. The blue box shows the main steps of the matching process performed by PPM and using a crossover operator. The purple box shows how PPM perturbs the conditional probabilities used in SIS

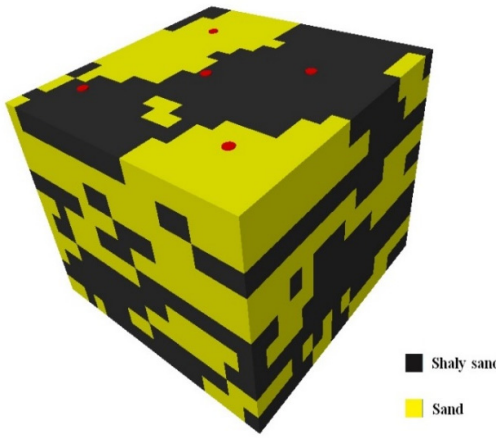

Figure 3. The reference (true) reservoir lithofacies model and locations of the pseudo-wells

The porosity and fluid saturation modeling process are performed concerning each lithofacies type. For each lithofacies type, a specific interval of porosity and fluid saturation is considered. The porosity values for sand and shaly sand are obtained from a Gaussian distribution with a mean of 0.18 and 0.04 and a standard deviation of 0.03 and 0.01, respectively. These distribution functions assign a range of (0.09-0.27) porosity values to sand (reservoir section) and a range of (0.01-0.07) to the shaly sand (non-reservoir section). The presence of shale particles between the sand grains reduces the storage capacity. Accordingly, the porosity values assigned to shaly sand are obviously less than sand. The water saturation values for sand and shaly sand are obtained from a uniform distribution with a range of [0.2-0.3] and [0.5-0.6], respectively. In non-reservoir sections (shaly sand) where shale is present between sand grains, the throats' radius reduces. As a result, capillary pressure increases and oil cannot enter these tiny pores. So, the assigned values of water saturation for shaly sand lithofacies are higher than the reservoir sandy parts. To take this into account, higher values of water saturation are assigned to shaly sands. The assigned porosity and water saturation values are assumed to be true measurements obtained from a perfect well-logging operation. The generated porosity and water saturation models for our synthetic case are shown in figures 4 and 5, respectively.

To produce P-wave impedance model (Figure 6), the petro-elastic model based on explained relationships in section 2.5 is applied on the reference reservoir lithofacies model. The generated P-wave acoustic impedance model (figure 6) is assumed to be the true impedance volumes which are resulted from a noise-free inversion of baseline seismic data.

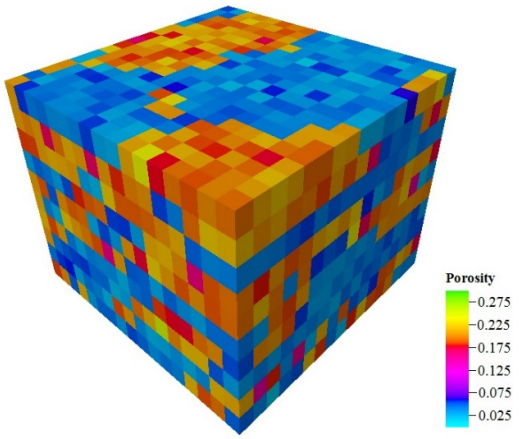

Figure 4. The reference porosity model which is generated by assigning an average porosity value to each lithofacies type

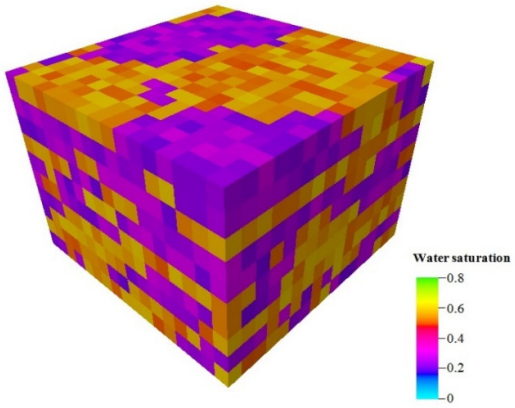

Figure5. The reference water saturation model built by assigning a known interval of water saturation values to each lithofacies type

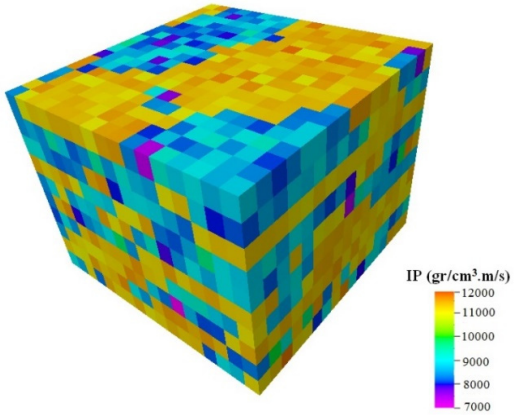

Figure 6. The reference (true) P-wave impedance model which is generated by applying a petro-elastic model on the reference reservoir model

In this study, none of the upscaling methods have been used because the well and seismic data are on the same scale. In real cases, upscaling is necessary since the data are on different scales; however, the synthetic case has been built in a way that the well and seismic data are on the same scale. The elastic properties of lithology types used in petro-elastic modeling are reported in Table 1.

Discussion

In this research, our proposed approach that aims at generating consistent reservoir lithofacies with well-log and P-wave impedance data is applied to a 3D test model. The purpose of using synthetic model is to verify and validate the proposed algorithm's capability in reference model's regeneration. Since our test model is a synthetic case, the reference model is known, as it is first generated and the other dataset (such as P-impedance) are produced based on this reference model. Next, this reference model has been put aside and the produced dataset is used to construct lithofacies models according to our proposed methodology. The final produced lithofacies models are compared with reference model to prove the efficiency of approach. Clearly, this kind of validation can only be performed on synthetic cases. To do so, the lithofacies indicators are assumed to be unknown in all grid blocks except those where the wells are located. In addition to the available data sources, information such as the variogram model, the porosity and fluids saturation average values, the elastic properties of lithology types, is accessible. With the reference lithofacies model in hand, the mismatch parameter can be used

to evaluate the accuracy of the constructed lithofacies models. The mismatch parameter is the average number of grid blocks in the constructed lithofacies model whose facies indicator is different from the corresponding grid blocks in the reference model. The lower the constructed models' mismatch values, the more similarity between the models and reference model, which means there is more consistency with the available datasets. After applying the proposed method to this specified problem, we found out that the mismatch values for 100 generated lithofacies models were in the range of (14.18)% to (17.09)%. One of the lithofacies models generated by the proposed approach is shown in Figure 7.

The most effective parameter on the final result is the weights considered for data sources in the equation (13). τ_1 and τ_2 are the weights intended for litho-logs and P-wave acoustic impedance, respectively. When a reference lithofacies model is in hand, the mismatch parameter can be a powerful tool for quantifying the algorithm's performance. Figure (8) shows τ_1 and τ_2 values' impact on the mismatch values.

Table1. Elastic properties of lithology types used in petro-elastic modeling

Lithology types	$G_m(GPa)$	$K_m(GPa)$	φ_c	$\rho_m(gr/cm^3)$
(Clean) sand	22	38	0.4	**2.6**
Shaly sand	15.5	30	0.5	**2.7**

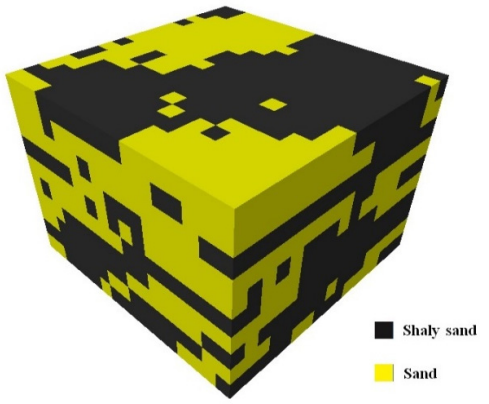

Figure 7. One of the reservoir lithofacies models generated by the proposed approach

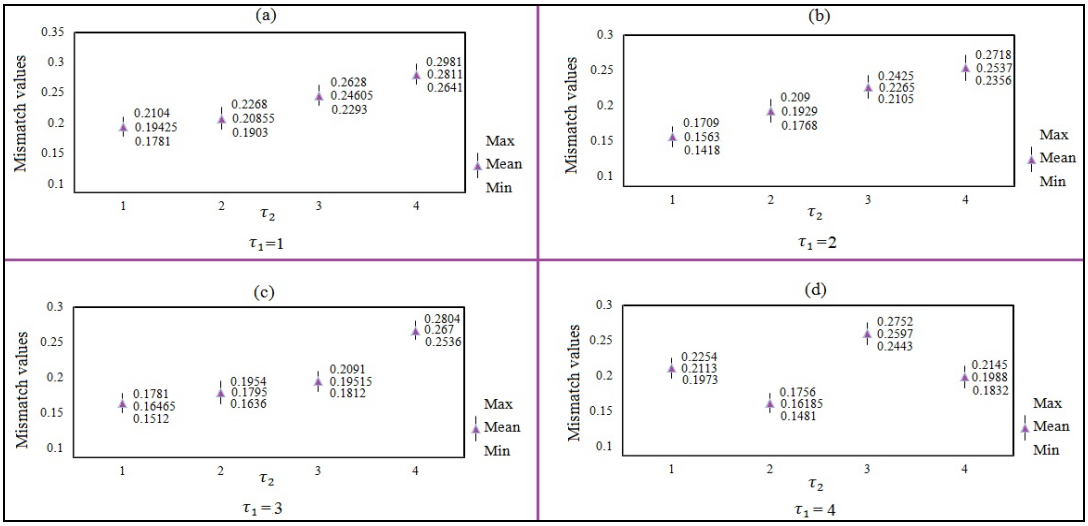

Figure 8. Impact of τ_1 and τ_2 values on mismatch of the generated lithofacies models for 15 independent algorithm runs. (a) $\tau_1 = 1$, $\tau_2 = \{1, 2, 3, 4\}$, (b) $\tau_1 = 2$, $\tau_2 = \{1, 2, 3, 4\}$ (c) $\tau_1 = 3$, $\tau_2 = \{1, 2, 3, 4\}$, and (d) $\tau_1 = 4$, $\tau_2 = \{1, 2, 3, 4\}$.

Figure 8 shows the mismatch values of the generated lithofacies models versus different values of τ_1 and τ_2. The obtained results illustrate that considering $\frac{\tau_1}{\tau_2} = 2$ ratio results in generating models associated with lower mismatch values in comparison with other ratios.

To show the effect of crossover operator on the obtained results, the problem is also solved by the proposed method without using the crossover operator. The results revealed that the mismatch values for generated lithofacies models is in the range of (18.58) % to (21.81) %. It means implementing of the crossover operator in the lithofacies modeling process results in a (4.565) % improvement (on average) in mismatch values of generated lithofacies models.

To highlight the capability of the proposed approach, two conventional geostatistical approaches were also applied to incorporate litho-logs and P-wave acoustic impedance in the lithofacies modeling process. These two approaches are constraining methods applied on SIS. In these methods, along with variogram parameters that are estimated from the litho-logs, extra constraints are defined based on the litho-logs and seismic data. These extra constraints improve the calculation accuracy of conditional probabilities used in SIS. The first constraining method, The Vertical Probability Trend, measures the lithofacies proportions (blue curve in Figure 9) from litho-log data in every layer of the reservoir. These lithofacies proportions are considered as a supplementary constraint to populate the lithofacies indicators in the whole reservoir framework.

The second constraining method, The Seismic Probability Trend method, simultaneously incorporate well-log and seismic data measured at borehole locations to determine a cross-plot of lithofacies indicators vs. seismic attribute values (P-wave impedance, in this study). Then the generated lithofacies realizations can be constrained by the produced P-wave impedance litho-probability curve (Figure 10).

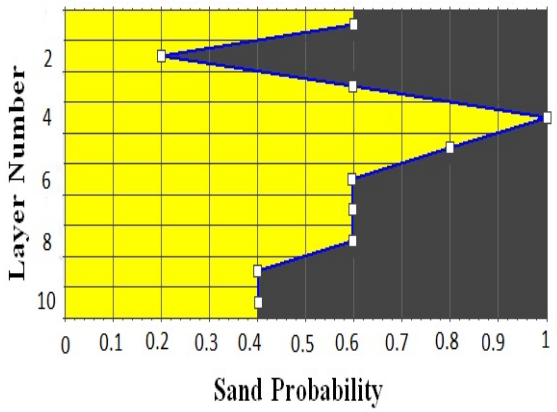

Figure 9. The probability distribution function generated by measuring the lithofacies proportions (blue curve) from litho-log data in each layer of the reservoir

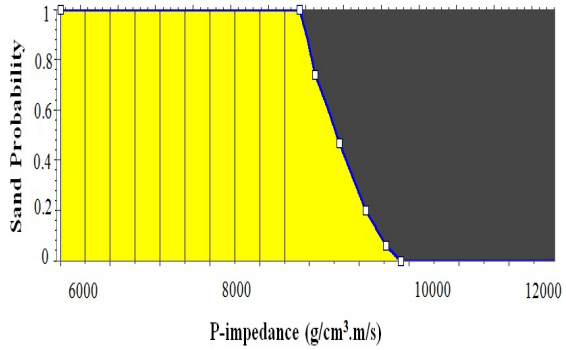

Figure 10. The probability distribution function generated by determining a cross-plot of lithofacies indicators vs. P-wave impedance of lithofacies indicators at borehole locations

One hundreds lithofacies models were generated by applying each of the mentioned constraining methods on SIS technique. The mismatch values for models generated by applying the Vertical Probability Trend and the Seismic Probability Trend were in the range of (35.82 - 43.05) % and (29.91 - 35.31) %, respectively. An example of these generated lithofacies models are shown in Figures 11 and 12.

The obtained results illustrate an adequate visual match between the reference lithofacies model and the generated lithofacies models via our proposed approach. Table 2 reports the quantitative information on the mismatch values for generated lithofacies models by the mentioned approaches.

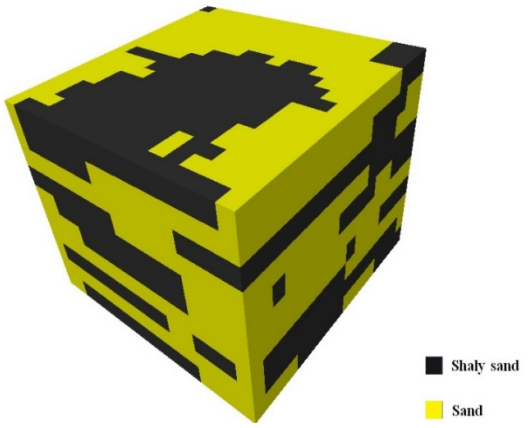

Figure 11. One of the reservoir lithofacies models generated by applying the constraining method of Vertical Probability Trend on SIS

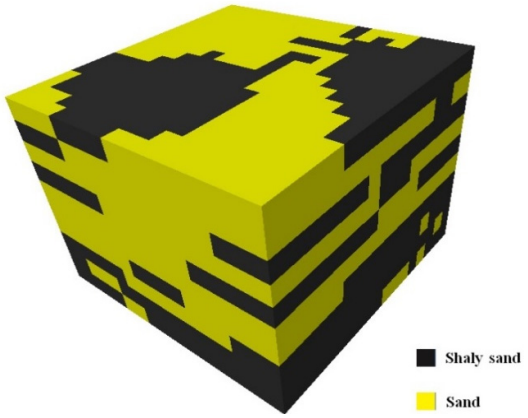

Figure 12. One of the reservoir lithofacies models generated by applying the constraining method of Seismic Probability Trend on SIS

Table2. The mismatch values of the generated lithofacies models compared to the reference model

	Applying the Vertical Probability Trend on SIS	**Applying the Seismic Probability Trend on SIS**	**Proposed approach without using the crossover operator**	**Proposed approach**
Mismatch values (%) for generated models compared to reference model (average)	[35.82-43.05] (39.43)	[29.91-35.31] (32.61)	[18.58-21.81] (20.195)	**[14.18-17.09] (15.63)**

Table 2 shows that using the proposed method was associated with an (23.8) % and (16.98) % improvement on mismatch values compared to the Vertical Probability Trend and Seismic Probability Trend constraining methods, respectively. This significant improvement indicates the superiority of the proposed method compared to the traditional geostatistical methods.

Conclusion

We introduced a new approach to integrate well and seismic data into the reservoir lithofacies modeling process. This approach is a combination of the sequential indicator simulation and the probability perturbation method within the Bayes' theorem framework. Implementation of the crossover operator enhanced the exploitation capability of the proposed approach. A 3D reservoir lithofacies model estimation problem is presented to validate the capability of the proposed approach. Qualitative and quantitative analysis of the obtained results demonstrate considerable improvement in matching the reservoir lithofacies models generated via our proposed approach with the reference lithofacies model, compared to the conventional geostatistical simulation techniques. In addition, the results revealed that including a crossover operator in the proposed algorithm gives a better matching of the generated reservoir lithofacies models with the reference model.

References

Abdel-Basset, M., Abdel-Fatah, L., Sangaiah, A.K., 2018. Metaheuristic algorithms: A comprehensive review. In Computational intelligence for multimedia big data on the cloud with engineering applications (pp. 185-231). Academic Press.

Abdel-Fattah, M.I., Pigott, J.D., El-Sadek, M.S., 2020. Integrated seismic attributes and stochastic inversion for reservoir characterization: Insights from Wadi field (NE Abu-Gharadig Basin, Egypt). Journal of African Earth Sciences, 161: 103661.

Abdelmaksoud, A., Amin, A.T., El-Habaak, G.H. and Ewida, H.F., 2019. Facies and petrophysical modeling of the Upper Bahariya Member in Abu Gharadig oil and gas field, north Western Desert, Egypt. Journal of African Earth Sciences, 149: 503-516.

Adelu, A.O., Aderemi, A.A., Akanji, A.O., Sanuade, O.A., Kaka, S.I., Afolabi, O., Olugbemiga, S., Oke, R., 2019. Application of 3D static modeling for optimal reservoir characterization. Journal of African Earth Sciences, 152: 184-196.

Agarwal, M., Srivastava, G.M.S., 2018. Genetic Algorithm-Enabled Particle Swarm Optimization (PSOGA)-Based Task Scheduling in Cloud Computing Environment. International Journal of Information Technology & Decision Making, 17(04): 1237-1267.

Angeleri, G.P., Carpi, R., 1982. Porosity prediction from seismic data. Geophysical prospecting, 30(5): 580-607.

Besag, J., Green, P.J., 1993. Spatial statistics and Bayesian computation. Journal of the Royal Statistical Society: Series B (Methodological), 55(1), pp.25-37.

Binitha, S., Sathya, S.S., 2012. A survey of bio inspired optimization algorithms. International journal of soft computing and engineering, 2(2):137-151.

Blum, C. and Roli, A., 2003. Metaheuristics in combinatorial optimization: Overview and conceptual comparison. ACM computing surveys (CSUR), 35(3), pp.268-308.

Bornard, R., Allo, F., Coleou, T., Freudenreich, Y., Caldwell, D.H., Hamman, J.G., 2005, June. Petrophysical Seismic Inversion to Determine More Accurate and Precise Reservoir Properties (SPE94144). In 67th EAGE Conference & Exhibition (pp. cp-1). European Association of Geoscientists & Engineers.

Bosch, M., Mukerji, T., Gonzalez, E.F., 2010. Seismic inversion for reservoir properties combining statistical rock physics and geostatistics: A review. Geophysics, 75(5): 75A165-75A176.

Caers, J. and Hoffman, T., 2006. The probability perturbation method: a new look at Bayesian inverse modeling. Mathematical geology, 38(1), pp.81-100.

Crawford, B., Soto, R., Astorga, G., García, J., Castro, C., Paredes, F., 2017. Putting continuous metaheuristics to work in binary search spaces. Complexity, 2017.

Churanova, N.Y., Chorniy, A.V., Baranov, T.S., Solovyev, A.V., Sadreev, E.A., Kurelenkov, S.K., Yudin, E.V., Danko, D.A., 2018, October. Reservoir Properties Distribution Based on Petroelastic Modeling PEM. In SPE Russian Petroleum Technology Conference. Society of Petroleum Engineers.

Doyen, P., 2007. Seismic reservoir characterization: An earth modelling perspective (2: 255). Houten: EAGE publications.

Elzain, H.E., Abdullatif, O., Senapathi, V., Chung, S.Y., Sabarathinam, C., Sekar, S., 2020. Lithofacies modeling of Late Jurassic in upper Ulayyah reservoir unit at central Saudi Arabia with inference of reservoir characterization. Journal of Petroleum Science and Engineering, 185, p.106664.

El Khadragy, A.A., Eysa, E.A., Hashim, A., El Kader, A.A., 2017. Reservoir characteristics and 3D static modelling of the Late Miocene Abu Madi Formation, onshore Nile Delta, Egypt. Journal of African Earth Sciences, 132: 99-108.

Emami Niri, M. and Lumley, D.E., 2015. Simultaneous optimization of multiple objective functions for reservoir modeling. Geophysics, 80(5): M53-M67.

Emami Niri, M., 2018. 3D and 4D Seismic Data Integration in Static and Dynamic Reservoir Modeling: A Review. Journal of Petroleum Science and Technology, 8(2): 38-56.

Emami Niri, M., Lumley, D.E., 2017. Initialising reservoir models for history matching using pre-production 3D seismic data: constraining methods and uncertainties. Exploration Geophysics, 48(1), pp.37-48.

Emami Niri, M., Lumley, D.E., 2016. Estimation of subsurface geomodels by multi-objective stochastic optimization. Journal of Applied Geophysics, 129: 187-199.

Niri, M.E. and Lumley, D., 2013, August. Uncertainty analysis in quantitative integration of inverted 3D seismic data for static reservoir modeling. In 13th International Congress of the Brazilian Geophysical Society & EXPOGEF, Rio de Janeiro, Brazil, 26–29 August 2013 (pp. 993-997). Society of Exploration Geophysicists and Brazilian Geophysical Society.

Galli, A., Beucher, H., 1997, January. Stochastic models for reservoir characterization: a user-friendly review. In Latin American and Caribbean Petroleum Engineering Conference. Society of Petroleum Engineers.

Garg, H., 2016. A hybrid PSO-GA algorithm for constrained optimization problems. Applied Mathematics and Computation, 274: 292-305.

Gassmann, F., 1951. Über die elastizität poröser medien: Vierteljahrss-chrift der Naturforschenden Gesellschaft in Zurich 96, 1-23. Paper translation at http://sepwww. stanford. edu/sep/berryman/PS/gassmann. pdf.

Grana, D. and Della Rossa, E., 2010. Probabilistic petrophysical-properties estimation integrating statistical rock physics with seismic inversion. Geophysics, 75(3): O21-O37.

Grana, D., Mukerji, T. and Dvorkin, J., 2011. Single loop inversion of facies from seismic data using sequential simulations and probability perturbation method. In SEG Technical Program Expanded Abstracts 2011 (pp. 1769-1773). Society of Exploration Geophysicists.

Grana, D., Mukerji, T., Dvorkin, J. and Mavko, G., 2012. Stochastic inversion of facies from seismic data based on sequential simulations and probability perturbation method. Geophysics, 77(4): M53-M72.

Hoffman, B.T., 2005. Geologically consistent history matching while perturbing facies.

Hoffman, B.T. and Caers, J., 2003, January. Geostatistical history matching using a regional probability perturbation method. In SPE Annual Technical Conference and Exhibition. Society of Petroleum Engineers.

Journel, A.G., Gomez-Hernandez, J.J., 1993. Stochastic imaging of the Wilmington clastic sequence. SPE formation Evaluation, 8(01): 33-40.

Journel, A.G., 2002. Combining knowledge from diverse sources: An alternative to traditional data independence hypotheses. Mathematical geology, 34(5): 573-596.

Kar, A.K., 2016. Bio inspired computing–a review of algorithms and scope of applications. Expert Systems with Applications, 59: 20-32.

Khajehzadeh, M., Taha, M.R., El-Shafie, A. and Eslami, M., 2011. A survey on meta-heuristic global optimization algorithms. Research Journal of Applied Sciences, Engineering and Technology, 3(6): 569-578.

Khormouji, H.B., Hajipour, H., Rostami, H., 2014, September. BODMA: a novel metaheuristic algorithm for binary optimization problems based on open source development model algorithm.

In 7'th International Symposium on Telecommunications (IST'2014) (pp. 49-54). IEEE.
Kim, K.H., Lee, K., Lee, H.S., Rhee, C.W., Shin, H.D., 2018. Lithofacies modeling by multipoint statistics and economic evaluation by NPV volume for the early Cretaceous Wabiskaw Member in Athabasca oilsands area, Canada. Geoscience Frontiers, 9(2): 441-451.
Koneshloo, M., Aryana, S.A., Grana, D., Pierre, J.W., 2017. A workflow for static reservoir modeling guided by seismic data in a fluvial system. Mathematical Geosciences, 49(8), pp.995-1020.
Mavko, G., Mukerji, T., 1998. A rock physics strategy for quantifying uncertainty in common hydrocarbon indicators. Geophysics, 63(6): 1997-2008.
Mavko, G., Mukerji, T. and Dvorkin, J., 1998. The rock physics handbook: Tools for seismic analysis in porous media: University of Cambridge.
Mondol, N.H., 2010. Seismic exploration. In Petroleum Geoscience (pp. 375-402). Springer, Berlin, Heidelberg.
Nur, A., Mavko, G., Dvorkin, J., Galmudi, D., 1998. Critical porosity: A key to relating physical properties to porosity in rocks. The Leading Edge, 17(3): 357-362.
Ravalec-Dupin, L., Enchery, G., Baroni, A. and Da Veiga, S., 2011. Preselection of reservoir models from a geostatistics-based petrophysical seismic inversion. SPE Reservoir Evaluation & Engineering, 14(05): 612-620.
Strebelle, S., 2002. Conditional simulation of complex geological structures using multiple-point statistics. Mathematical geology, 34(1): 1-21.
Tang, M., Lu, S., Zhang, K., Yin, X., Ma, H., Shi, X., Liu, X., Chu, C., 2019. A three dimensional high-resolution reservoir model of Napo Formation in Oriente Basin, Ecuador, integrating sediment dynamic simulation and geostatistics. Marine and Petroleum Geology, 110: 240-253.
Tewari, S., Dwivedi, U.D., 2019. Ensemble-based big data analytics of lithofacies for automatic development of petroleum reservoirs. Computers & Industrial Engineering, 128: 937-947.
Wood, A.B., 1941. A textbook of sound: Bell.
Zhang, Z., Li, H., Zhang, D., 2017. Reservoir characterization and production optimization using the ensemble-based optimization method and multi-layer capacitance-resistive models. Journal of Petroleum Science and Engineering, 156: 633-653.